Two Approaches for Guaranteed State Estimation of Nonlinear Continuous-Time Models

Marco Kletting, Michel Kieffer, Eric Walter

Two Approaches for Guaranteed State Estimation of Nonlinear Continuous-Time Models

Marco Kletting, Michel Kieffer (✉), and Eric Walter

Abstract This paper deals with the estimation of the state vector of a nonlinear continuous-time state-space model, such as those frequently encountered in the context of knowledge-based modeling. Unknown and possibly time-varying parameters may be included in an extended state vector to deal with the simultaneous estimation of state and parameters. Observations depending on the (possibly extended) state are assumed to take place at discrete measurement times. Given bounds on the size of the additive measurement errors, guaranteed estimation should then provide bounds on the possible values of the state at any given time. Two recently developed approaches are presented and their performance is compared on a simple test case.

1 Introduction

When building knowledge-based models, for instance models based on the laws of physics, one frequently ends up with a continuous-time state-space model, which may depend on a possibly time-varying vector of parameters $\mathbf{p} \in \mathbb{R}^{n_p}$:

$$\dot{\mathbf{x}}(t) = \mathbf{f}_x\left(\mathbf{x}(t), \mathbf{p}(t)\right),$$

Marco Kletting
Multi-Function Airborne Radars (OPES22), Cassidian Electronics,Woerthstr. 85, 89077 Ulm, Germany e-mail: marco.kletting@cassidian.com

Michel Kieffer
Laboratoire des Signaux et Systèmes - CNRS - SUPELEC - Univ Paris-Sud, 3 rue Joliot-Curie, F-91192 Gif-sur-Yvette cedex, on leave at LTCI - CNRS - Telecom ParisTech, 46 rue Barault, F-75013 Paris e-mail: michel.kieffer@lss.supelec.fr

Eric Walter
Laboratoire des Signaux et Systèmes - CNRS - SUPELEC - Univ Paris-Sud, 3 rue Joliot-Curie, F-91192 Gif-sur-Yvette cedex e-mail: eric.walter@lss.supelec.fr

where $\mathbf{x} \in \mathbb{R}^{n_x}$ is the state vector. Provided that an equation is specified for the dynamics of $\mathbf{p}$, such as

$$\dot{\mathbf{p}}(t) = \Delta\mathbf{p} \quad \text{with} \quad \Delta\mathbf{p} \in [\Delta\underline{\mathbf{p}}, \Delta\overline{\mathbf{p}}],$$

one can concatenate the state and parameter vectors into an extended state vector $\mathbf{z}(t) = [\mathbf{x}(t)^T, \mathbf{p}(t)^T]^T$. Then

$$\dot{\mathbf{z}}(t) = \mathbf{f}(\mathbf{z}(t)), \tag{1}$$

where

$$\mathbf{f} = \begin{bmatrix} \mathbf{f}_x(\mathbf{x}(t), \mathbf{p}(t)) \\ \Delta\mathbf{p} \end{bmatrix}$$

with $\mathbf{f} : D \mapsto \mathbb{R}^n$, $D \subset \mathbb{R}^n = \mathbb{R}^{n_x} \times \mathbb{R}^{n_p}$. Any time-invariant parameter p_i should satisfy $\Delta p_i = 0$.

This paper is devoted to the estimation of the state of such a model from discrete-time measurements. Measurement times $t_1 < t_2 < \cdots < t_{k_{max}}$ may not be regularly spaced. The step from t_k to t_{k+1}, with size $h_k = t_{k+1} - t_k$, is referred to as the $(k+1)$-st step. The vector $\mathbf{y}(t_k) \in \mathbb{R}^m$ of the values measured at time t_k is assumed to satisfy

$$\mathbf{y}(t_k) = \check{\mathbf{y}}(t_k) + \delta(t_k), \tag{2}$$

where $\delta(t_k)$ is an additive measurement error vector and

$$\check{\mathbf{y}}(t_k) = \mathbf{h}\left(\mathbf{z}\left(t_k\right), t_k\right) \tag{3}$$

is the result that would have been obtained from ideal measurements. Usually, $n < m$. The absolute value of the measurement error is assumed to be bounded, with a known upper bound $\overline{\delta}$, which implies that $\delta(t_k) \in [-\overline{\delta}; \overline{\delta}]$ for all k. As a result, we have

$$\check{\mathbf{y}}(t_k) \in [\mathbf{y}(t_k)] = [\mathbf{y}(t_k) - \overline{\delta}, \mathbf{y}(t_k) + \overline{\delta}] \ .$$

If there are uncertain parameters in the measurement equation, then they can be incorporated in the extended state vector, just as we have done with the uncertain parameters in the state equation. In what follows, we shall therefore only be concerned with the computation of guaranteed estimates of the (extended) state vector, which contain guaranteed estimates of the parameters of the state and observation equations, if any. This is why the extended state will simply be called state in what follows, unless we need to distinguish the parameters from the state proper.

Guaranteed nonlinear state estimation in this context of bounded-measurement errors have been addressed by a number of authors, see *e.g.* [2, 3, 7, 10, 15, 16, 22, 23, 26, 27, 30, 32]. All these approaches enclose the set of all state values consistent with the model, and the measurements and noise bounds. They differ first by the wrappers used to perform enclosure. Ellipsoids are used in [2, 3, 16, 30], zonotopes in [15], boxes in [7, 10, 22, 23, 26, 27], and union of boxes in [32]. A second important difference is in the hypotheses about the measurements. In [22, 23, 27], continuous-time measurements are assumed to be available. This rather unrealistic assumption allows nice convergence properties of the estimators to be obtained.

Here, discrete-time measurements will be considered, which appears more realistic, but makes convergence analysis much more difficult, especially for nonlinear systems. Techniques using boxes or union of boxes as wrappers usually rely on interval analysis and guaranteed integration of ODEs.

We shall assume in this chapter that bounds are available on the possible value of the initial state, and that estimates of the present state are to be produced based on the past measurements only. As for most state estimators including the celebrated Kalman filter, the $(k+1)$-st step of the procedure will then consist of two steps: a *prediction step* that predicts the evolution of the state between two instants of time at which measurements are obtained, and a *correction step* during which the newly acquired data are taken into account to reduce the uncertainty in the result of the prediction step. In the context of guaranteed estimation, the prediction step involves guaranteed integration under consideration of all uncertainties, and the correction step must eliminate any part of the predicted set that can be proved to be inconsistent with the new measurements given the bounds on the measurement errors. For the sake of simplicity, no state perturbation has been considered here. On how state perturbations may be considered, see, *e.g.*, [12].

Section 2 overviews bounded-error state estimation in an idealized context. Section 3 considers two approaches that rely on interval analysis and try to counteract the pessimism of guaranteed integration when the initial conditions are uncertain, as is the case in an estimation context. The first of these approaches is based on Müller's theorem and presented in Section 3.1, while the second, based on the use of high-order Taylor models is described in Section 3.2. Various ways to implement correction steps are then described in Section 4. The resulting algorithms are compared in Section 5 on a simple test-case.

2 Idealized State Estimation

Let $\mathbb{Z}(t)$ be the set of all state values that are consistent with the information available up to time t. An idealized bounded-error counterpart of the Kalman filter for nonlinear discrete-time systems, alternating prediction and correction steps [8], may be considered to build $\mathbb{Z}(t)$ at each t.

If $\mathbf{z}(t_k)$ at t_k is only known to belong to $\mathbb{Z}(t_k)$, the *set* of solutions at time $t > t_k$ of (1) is

$$\mathbf{z}(t;t_k,\mathbb{Z}(t_k)) = \{\mathbf{z}(t;t_k,\mathbf{z}(t_k)) \mid \mathbf{z}(t_k) \in \mathbb{Z}(t_k)\}\,.$$

For the $(k+1)$-st prediction step, one has thus to compute the *predicted* set

$$\mathbb{Z}^+(t_{k+1}) = \mathbf{z}(t_{k+1};t_k,\mathbb{Z}(t_k)).$$

For the $(k+1)$-st correction step, one has to take into account the measurement available at time t_{k+1} to update $\mathbb{Z}^+(t_{k+1})$ and obtain

$$\mathbb{Z}(t_{k+1}) = \left\{\mathbf{z} \in \mathbb{Z}^+(t_{k+1}) \,|\, \mathbf{h}\,(\mathbf{z},t_{k+1}) \in [\mathbf{y}(t_{k+1}) - \overline{\boldsymbol{\delta}}, \mathbf{y}(t_{k+1}) + \overline{\boldsymbol{\delta}}]\right\}, \qquad (4)$$

thus $\mathbb{Z}(t_{k+1}) \subseteq \mathbb{Z}^+(t_{k+1})$.

Provided that all hypotheses on the state equation and the measurement noise are satisfied, $\mathbb{Z}(t_{k+1})$ does contain $\mathbf{z}(t_{k+1})$. The main difficulty in this idealized algorithm comes from the fact that $\mathbb{Z}(t_k)$ may have a quite complex shape. Outer-approximations of the sets $\mathbb{Z}$ and $\mathbb{Z}^+$ have thus to be evaluated. These outer-approximations may consist of interval vectors (boxes), union of non-overlapping boxes (subpavings), or may be described using Taylor models. Implementable counterparts of the idealized prediction and correction steps are now described.

3 Prediction Step

A naive approach to obtain an outer-approximation for $\mathbf{z}(t_k;t_0,[\mathbf{z}(0)])$, $k = 1 \ldots k_{max}$, would be to use one of the guaranteed ODE solvers based on interval analysis `AWA` [18], `VNODE` [25], `COSY IV` [6], `VSPODE` [17], or `ValEncIA-IVP` [28,29]. The main difficulty is to obtain accurate enclosures for the solutions, when there are uncertain parameters, bounded state perturbation, or uncertain initial conditions.

One may enclose the solutions of (1) with *uncertain* initial conditions between a pair of coupled system of ODEs with *deterministic* initial conditions using Müller's theorem [24]. Other types of uncertainty may be taken into account as well, such as unknown but bounded inputs. Any guaranteed tool for solving ODEs may then be used to solve this system, see Section 3.1.

When only the initial conditions are undetermined, but known to belong to some box, guaranteed ODE solvers such as `COSY IV`, `VSPODE`, or `ValEncIA-IVP` perform quite well, since they are evaluating a Taylor development of the solution with interval remainder, this developments being made also with respect to the initial condition, see Section 3.2.

3.1 Using Müller's Theorem

Here, the solution is obtained by bounding the solutions of dynamical systems with *uncertain* parameters or initial conditions using *deterministic* dynamical systems. This approach has been previously presented in [11, 31] in the context of cooperative dynamical models, *i.e.*, models such as (1) for which the off-diagonal terms of the Jacobian matrix of $\mathbf{f}$ are positive. These results were inspired by the interval observer proposed in [5]. Müller's theorems [24], which have recently been used in the context of guaranteed simulation [4], make it possible to bound the solutions of more general dynamical models, see also [13].

3.1.1 Müller's Theorem

The following theorem [24] may be directly applied to bound the solutions of dynamical models such as (1) in the presence of uncertain initial conditions $\mathbf{z}(t_k) \in [\mathbf{z}(t_k)]$, where $[\mathbf{z}(t_k)]$ is a box in state space.

Theorem 1. *Assume that* $\mathbf{f}(\mathbf{z}(t))$ *in* (1) *is continuous on*

$$\mathbb{T} : \begin{cases} \omega(t) \leqslant \mathbf{x} \leqslant \Omega(t) \\ t_k \leqslant t \leqslant t_{k+1} \end{cases}$$

where $\omega_i(t)$ *and* $\Omega_i(t)$, $i = 1 \ldots n_x$, *are continuous on* $[t_k, t_{k+1}]$ *and satisfy*

1. $\omega(t_k) = \underline{\mathbf{z}}(t_k)$ *and* $\Omega(t_k) = \overline{\mathbf{z}}(t_k)$,
2. *the left derivatives* $D^- \omega_i(t)$ *and* $D^- \Omega_i(t)$ *and right derivatives* $D^+ \omega_i(t)$ *and* $D^+ \Omega_i(t)$ *of* $\omega_i(t)$ *and* $\Omega_i(t)$ *satisfy, for* $i = 1 \ldots n$ *and all* $t \in [t_k, t_{k+1}]$,

$$D^{\pm} \omega_i(t) \leqslant \min_{\underline{\mathbb{T}}_i(t)} f_i(\mathbf{z}) \qquad \text{and} \qquad D^{\pm} \Omega_i(t) \geqslant \max_{\overline{\mathbb{T}}_i(t)} f_i(\mathbf{z}),$$

where $\underline{\mathbb{T}}_i(t)$ *is the subsets of D defined by*

$$\underline{\mathbb{T}}_i(\tau) : \begin{cases} z_i = \omega_i(\tau), \\ \omega_j(\tau) \leqslant z_j \leqslant \Omega_j(\tau), \ j \neq i, \\ t = \tau, \end{cases}$$

and $\overline{\mathbb{T}}_i(t)$ *is the subset of D defined by*

$$\overline{\mathbb{T}}_i(\tau) : \begin{cases} z_i = \Omega_i(\tau) \\ \omega_j(\tau) \leqslant z_j \leqslant \Omega_j(\tau), \ j \neq i, \\ t = \tau. \end{cases}$$

Then, for any given $\mathbf{z}(t_k) \in [\mathbf{z}(t_k)]$, *a solution to* (1) *exists, such that*

$$\omega(t) \leqslant \mathbf{z}(t) \leqslant \Omega(t) \quad \forall t \in [t_k, t_{k+1}],$$

and this solution is equal to $\mathbf{z}(t_k)$ *at* $t = t_k$. *Moreover, if for any* $t \in [t_k, t_{k+1}]$, $\mathbf{f}(\mathbf{z}, t)$ *is Lipschitz with respect to* $\mathbf{z}$, *then for any given* $\mathbf{z}(t_k) \in [\mathbf{z}(t_k)]$ *this solution is unique.* $\diamondsuit$

The main idea of this theorem is to bracket the solutions of (1) between the solution of two deterministic ODEs. The initial conditions for these ODEs are given by 1. and the conditions that have to be satisfied by each solution are given by 2., see Section 5 for an example.

3.1.2 Prediction Step Using Müller's Theorem

Müller's theorem allows the evaluation of lower and upper bounds for the solution of (1) provided that two functions $\omega(t)$ and $\Omega(t)$ are available. The interval function $[\Phi](t) = [\omega(t), \Omega(t)]$ can then be seen as an *inclusion function* for all solutions $\mathbf{z}(t)$ of the state equation in (1).

$[\Phi](t)$ provides a *box* containing the state at each time instant. More accurate descriptions of the predicted set may be obtained by *splitting* the box corresponding to the initial conditions into non-overlapping subboxes, and to apply Müller's theorem on each of the resulting subboxes. A list of overlapping boxes is obtained, which may be merged into a subpaving using the `ImageSp` algorithm [8]. This subpaving may then be used by any implementable correction step described in Section 4, or used to perform a new prediction until a measurement is available. The accuracy of the description of $\mathbb{Z}^+(t_k)$ at time t_k depends on some precision parameter ε, which determines the size of the boxes obtained after splitting the initial box or subpaving used by the `ImageSp` algorithm.

The construction of $\omega(t)$ and $\Omega(t)$ is usually easy on a case-by-case basis, as illustrated in Section 5.1. For more complex systems, hybrid automata may be put at work to build these functions, as detailed in [21].

An inclusion function for $\mathbf{h}$ may similarly be obtained using the sensitivity functions of the output with respect to the state, see Section 4.2.3.

3.2 Verified Integration Based on Taylor Models

Verified integration techniques such as `VNODE` [25] are based on a Taylor series expansion in time. `COSY-VI` [1] performs, in addition to this expansion in time, an expansion with respect to the initial state vector, denoted by $\mathfrak{z}$ in what follows. The box to which $\mathfrak{z}$ is assumed to belong is given by $[\mathfrak{z}]$. The expansion point with respect to the initial state vector $\mathfrak{z}$ is some $\hat{\mathfrak{z}} \in [\mathfrak{z}]$, and the expansion point with respect to time is t_k. The flow of the differential equation in a given time interval $[t_k, t_{k+1}]$ is enclosed by a n-dimensional Taylor model

$$\begin{aligned} &\mathbf{T}_\rho(\mathfrak{z}-\hat{\mathfrak{z}}, t-t_k) := \mathbf{P}_\rho(\mathfrak{z}-\hat{\mathfrak{z}}, t-t_k) + \mathbf{I}_{\rho,k+1}, \\ &\text{with} \quad \mathfrak{z} \in [\mathfrak{z}] \quad \text{and} \quad t \in [t_k, t_{k+1}] \ , \end{aligned}$$

where $\mathbf{P}_\rho(\mathfrak{z}-\hat{\mathfrak{z}}, t-t_k)$ is the multivariate polynomial part of order ρ and $\mathbf{I}_{\rho,k+1}$ is the remainder box. The i-th entry of the n-dimensional vector $\mathbf{T}_\rho(\mathfrak{z}-\hat{\mathfrak{z}}, t-t_k)$ is denoted by $T_{\rho,i}(\mathfrak{z}-\hat{\mathfrak{z}}, t-t_k)$. The Taylor model at $t = t_{k+1}$ is written as

$$\mathbf{T}_{\rho,k+1}(\mathfrak{z}-\hat{\mathfrak{z}}) := \mathbf{P}_{\rho,k+1}(\mathfrak{z}-\hat{\mathfrak{z}}) + \mathbf{I}_{\rho,k+1} \ .$$

The i-th entry of $\mathbf{T}_{\rho,k+1}(\mathfrak{z}-\hat{\mathfrak{z}})$ is given by $T_{\rho,i,k+1}(\mathfrak{z}-\hat{\mathfrak{z}})$.

Verified integration methods that use a single box or a single parallelepiped for the state enclosure may suffer from large overestimation, especially for nonlinear systems. The flow representation by Taylor models makes it possible to obtain tight enclosures of non-convex sets and leads to less overestimation.

The integral form of the differential equation (1) is given by

$$\mathscr{O}(\mathbf{z}(t)) := \mathbf{z}(t_k) + \int_{t_k}^{t} \mathbf{f}(\mathbf{z}(t'),t')dt'$$

Applying $\mathscr{O}$ to a Taylor model for the integration in the time-interval $[t_k, t_{k+1}]$ yields

$$\mathscr{O}(\mathbf{P}_\rho(\mathfrak{z}-\hat{\mathfrak{z}},t-t_k)+\mathbf{I}_{\rho,k+1}) = \mathbf{z}(t_k) + \int_{t_k}^{t} \mathbf{f}(\mathbf{P}_\rho(\mathfrak{z}-\hat{\mathfrak{z}},t'-t_k)+\mathbf{I}_{\rho,k+1})dt',$$

where $\mathbf{z}(t_k)$ is represented by its Taylor model enclosure at $t = t_k$.

$$\mathbf{T}_{\rho,k} = \mathbf{P}_{\rho,k}(\mathfrak{z}-\hat{\mathfrak{z}}) + \mathbf{I}_{\rho,k} \quad .$$

This leads to

$$\begin{aligned}&\mathscr{O}(\mathbf{P}_\rho(\mathfrak{z}-\hat{\mathfrak{z}},t-t_k)+\mathbf{I}_{\rho,k+1})\\ &= \mathbf{P}_{\rho,k}(\mathfrak{z}-\hat{\mathfrak{z}}) + \mathbf{I}_{\rho,k} + \int_{t_k}^{t} \mathbf{f}(\mathbf{P}_\rho(\mathfrak{z}-\hat{\mathfrak{z}},t-t_k)+\mathbf{I}_{\rho,k+1})dt'.\end{aligned}$$

The goal for the integration from t_k to t_{k+1} consists in determining a Taylor model $\mathbf{T}_\rho(\mathfrak{z}-\hat{\mathfrak{z}},t-t_k)$ such that

$$\mathscr{O}(\mathbf{P}_\rho(\mathfrak{z}-\hat{\mathfrak{z}},t-t_k)+\mathbf{I}_{\rho,k+1}) \subset \mathbf{P}_\rho(\mathfrak{z}-\hat{\mathfrak{z}},t-t_k)+\mathbf{I}_{\rho,k+1}$$

$\forall \mathfrak{z} \in [\mathfrak{z}]$ and $\forall t \in [t_k, t_{k+1}]$. The polynomial part and the interval remainder are determined in separate steps. A detailed description of these steps is given in [1, 14].

For numerical and implementation reasons it is advantageous to have the unit box $[-1;1]^n$ as the domain box in each integration step [20]. Thus the initial enclosure $[\mathbf{z}(0)]$ of the extended state vector $\mathbf{z}(t)$ is expressed as a Taylor model according to

$$\begin{aligned}[\mathbf{z}(0)] = \mathbf{T}(\mathfrak{z}) &= \mathbf{c} + \mathbf{D}\,\mathfrak{z}\\ \text{with} \quad &\mathfrak{z}_i \in [-1;1],\ \ i = 1\ldots n,\end{aligned}$$

where $\mathbf{c}$ is the midpoint of $[\mathbf{z}(0)]$ and $\mathbf{D}$ is a diagonal matrix with $d_{i,i} = \mathrm{rad}([\mathbf{z}(0)])$.

The expansion in initial state reduces the overestimation that may occur during integration. To limit the long-term growth of the remainder error and to reduce overestimation the following strategies can be applied:

- Shrink Wrapping: the interval remainder is absorbed in the polynomial part [20].
- Preconditioning: the ODE solution is studied in a more suitable coordinate system [19].
- Splitting: the domain box $[\mathfrak{z}]$ is split into subboxes and the enclosure of $\mathbf{z}(t)$ is given by a list of Taylor models [14]. This is described in the following section.

3.2.1 Splitting the Domain Box

As when using Müller's theorem, splitting of the domain box into subboxes [14] may be useful to reduce overestimation. The state vector $\mathbf{z}_{k+1}$ at $t = t_{k+1}$ is then enclosed by a list $\mathscr{T}_{k+1}$ of Taylor models

$$\mathbf{z}_{k+1} \in \mathscr{T}_{k+1} = \left\{ \mathbf{T}^{(1)}_{\rho,k+1}(\mathfrak{z}), \mathbf{T}^{(2)}_{\rho,k+1}(\mathfrak{z}) \dots \mathbf{T}^{(L_{k+1})}_{\rho,k+1}(\mathfrak{z}) \right\}$$
$$\text{with} \quad \mathfrak{z}_i = [-1;1], \quad i = 1 \dots n \quad \text{and} \quad L_{k+1} \leq L_{max}.$$

where L_{max} is the maximum allowed number of Taylor models. Consider a Taylor model $\mathbf{T}_{\rho,k+1}(\mathfrak{z})$ with the domain box $[\mathfrak{z}]$, $\mathfrak{z} \in [\mathfrak{z}]$. The domain box of this Taylor model is split into subboxes $[\mathfrak{z}^{(l)}]$, $l = 1 \dots L$,

$$\bigcup_{l=1}^{L} [\mathfrak{z}^{(l)}] = [\mathfrak{z}] \ .$$

To obtain again the unit box as a domain box, $[\mathfrak{z}^{(l)}]$ is expressed as a Taylor model according to

$$[\mathfrak{z}^{(l)}] = \widetilde{\mathbf{T}}^{(l)}(\mathfrak{z}) = \mathbf{c}^{(l)} + \mathbf{D}^{(l)}\,\mathfrak{z}$$
$$\text{with} \quad \mathfrak{z}_i \in [-1;1] \ , i = 1 \dots n \ ,$$

where $\mathbf{c}^{(l)}$ is the midpoint of $[\mathfrak{z}^{(l)}]$ and $\mathbf{D}^{(l)}$ is a diagonal matrix with $d^{(l)}_{i,i} = \mathrm{rad}([\mathfrak{z}^{(l)}_i])$. The components of the original initial state vector $\mathfrak{z}$ of $\mathbf{T}_{\rho,k+1}(\mathfrak{z})$ are replaced by the components of $\widetilde{\mathbf{T}}^{(l)}(\mathfrak{z})$ by substituting $\widetilde{T}^{(l)}_i(\mathfrak{z})$ for $\mathfrak{z}_i$, which results in a modified Taylor model

$$\mathbf{T}^{(l)}_{\rho,k+1}(\mathfrak{z}) = \mathbf{T}_{\rho,k+1}(\widetilde{\mathbf{T}}^{(l)}(\mathfrak{z}))$$

for each subbox $[\mathfrak{z}^{(l)}]$.

To determine the component in which the domain box has to be split, splitting criteria have to be evaluated for the considered Taylor model $\mathbf{T}_{\rho,k+1}(\mathfrak{z})$. Splitting is carried out perpendicularly to the direction which has been calculated by the spliting criteria. Approaches to determine the splitting direction are described in [14].

If several Taylor models are already present, the most appropriate Taylor model for the splitting has to be selected. This is done by calculating the interval enclosure of each Taylor model and the corresponding pseudo volume of the resulting box. The pseudo volume of a n-dimensional interval vector is calculated by the multiplication of the interval diameters of all its components. The Taylor model with the largest pseudo volume is selected. Alternatively, the Taylor model with the largest interval remainder could be selected.

How splitting of the domain box is combined with preconditioning is described in detail in [14].

3.2.2 Prediction Step Using Taylor Models

At time t_k, the extended state vector is enclosed by a list $\mathscr{T}_k$ of Taylor models

$$\mathbf{z}_k \in \mathscr{T}_k = \left\{ \mathbf{T}_{\rho,k}^{(1)}(\mathfrak{z}), \mathbf{T}_{\rho,k}^{(2)}(\mathfrak{z}) \dots \mathbf{T}_{\rho,k}^{(L_k)}(\mathfrak{z}) \right\}$$
$$\text{with} \quad \mathfrak{z}_i = [-1;1], \quad i = 1 \dots n \quad \text{and} \quad L_k \leq L_{max}.$$

First a Taylor model is selected for splitting, then a splitting criterion is evaluated, and the Taylor model is split by splitting the domain box in subboxes. Taylor models are split until a pre-specified number of Taylor models or number of splittings is reached. Next, for each Taylor model a verified integration is performed.

The resulting enclosure of the extended state vector at time t_{k+1} (after the prediction step) is then given by

$$\mathscr{T}_{k+1}^{pr} = \left\{ \mathbf{T}_{\rho,k+1}^{(pr,1)}(\mathfrak{z}), \mathbf{T}_{\rho,k+1}^{(pr,2)}(\mathfrak{z}) \dots \mathbf{T}_{\rho,k+1}^{(pr,L_{k+1}^{pr})}(\mathfrak{z}) \right\}$$
$$\text{with} \quad \mathfrak{z}_i = [-1;1], \quad i = 1 \dots n \quad \text{and} \quad L_{k+1}^{pr} \leq L_{max}.$$

The prediction step is repeated until measurements become available. The result of the last prediction step before measurements become available is used as an initial enclosure of the next correction step.

4 Correction Step

Assume that the prediction step at time t_{k+1} has produced a set $\mathbb{Z}^+(t_{k+1})$ that contains $\mathbf{z}(t_{k+1})$. This set may consist of a single box, a list of potentially overlapping boxes, or may be a subpaving.

The measurement vector $\mathbf{y}(t_{k+1})$ obtained at time t_{k+1} has now to be taken into account. Several practical implementations of the idealized correction step (4) are now presented.

4.1 Using Set Inversion Via Interval Analysis

The aim of the Set Inverter Via Interval Analysis (`SIVIA`) algorithm [9] is to eliminate parts of $\mathbb{Z}^+(t_{k+1})$ that can be proved to be inconsistent with the measurements, the measurement equation and the bounds on the measurement noise.

Consider a box $[\mathbf{z}] \subset \mathbb{Z}^+(t_{k+1})$. If $\mathbf{h}([\mathbf{z}], t_{k+1}) \subset [\mathbf{y}(t_{k+1}) - \overline{\delta}, \mathbf{y}(t_{k+1}) + \overline{\delta}]$, then all $\mathbf{z} \in [\mathbf{z}]$ are consistent with the measurements, model, and noise bounds. Therefore, $[\mathbf{z}]$ has been proved to belong to $\mathbb{Z}(t_{k+1})$. If $\mathbf{h}([\mathbf{z}], t_{k+1}) \cap [\mathbf{y}(t_{k+1}) - \overline{\delta}, \mathbf{y}(t_{k+1}) + \overline{\delta}] = \emptyset$, then no $\mathbf{z} \in [\mathbf{z}]$ is consistent with the measurement, model and noise bounds.

Thus, $[\mathbf{z}]$ has an empty intersection with $\mathbb{Z}(t_{k+1})$ and can be rejected. If none of the previous conditions is satisfied, $[\mathbf{z}]$ is said undetermined, as parts of $[\mathbf{z}]$ may belong to $\mathbb{Z}(t_{k+1})$.

The SIVIA algorithms iteratively performs selection, elimination, or bisection of boxes, starting from a large initial search box, list of boxes or subpaving. Undetermined boxes are bisected until their width is smaller than some precision parameter ε, which helps to trade-off complexity and accuracy of representation of the solution set, $\mathbb{Z}(t_{k+1})$ here. The solution provided by SIVIA is a subpaving, consisting of inner boxes and undetermined boxes deemed too small to be further bisected. This subpaving may be fed to the next prediction step. See [8] for more details and implementation issues.

4.2 Using Contractors

Bounded-error measurements translate into vector inequality constraint $\mathbf{k}(\mathbf{z}) \geqslant \mathbf{0}$, to be understood componentwise. A *contractor* $C_{\mathbf{k}}$ for $\mathbf{z}$ is an algorithm to compute a box $C_{\mathbf{k}}([\mathbf{z}])$ such that

$$\begin{cases} C_{\mathbf{k}}([\mathbf{z}]) \subset [\mathbf{z}], \\ \{\mathbf{z} \in [\mathbf{z}] \,|\mathbf{k}(\mathbf{z}) \geqslant \mathbf{0}\} \subset C_{\mathbf{k}}([\mathbf{z}]). \end{cases} \tag{5}$$

The first relation in (5) ensures that $[\mathbf{z}]$ is contracted, while the second guarantees that no value of $\mathbf{z}$ satisfying the constraints is lost. Contractors can be similarly defined in the case of equality constraints.

4.2.1 Improving the State Estimate

Given the measurement equations (2), (3) and the fact that $\delta_k \in \left[-\overline{\delta}, \overline{\delta}\right]$, two constraints may be obtained that have to be satisfied by the state vector at time t_k, namely

$$\mathbf{k}_1(\mathbf{z}) = \mathbf{y}(t_k) - \mathbf{h}(\mathbf{z}, t_k) + \overline{\delta} \geqslant \mathbf{0}$$

and

$$\mathbf{k}_2(\mathbf{z}) = -\mathbf{y}(t_k) + \mathbf{h}(\mathbf{z}, t_k) + \overline{\delta} \geqslant \mathbf{0}.$$

Various types of contractors may be considered [8], depending on the structure of $\mathbf{h}(\mathbf{z}, t_k)$. If $m = n$, the interval Newton or the Krawczyk contractors may be employed.

4.2.2 Improving the Initial Conditions Estimate

If one is interested in obtaining a better estimate of the initial conditions, one may write $\mathbf{h}(\mathbf{z},t_k)$ as a function of $\mathfrak{z}$. For that purpose, consider the i-th entry of $\mathbf{h}(\mathbf{z},t_k)$. We have

$$h_i([\mathbf{z}_{k+1}],t_k) \subset h_i([\mathbf{z}_{k+1}](\widehat{\mathfrak{z}}),t_k) + ([\mathfrak{z}]-\widehat{\mathfrak{z}})^{\mathrm{T}} \left.\frac{\partial h_i(\mathbf{z},t_k)}{\partial \mathfrak{z}}\right|_{[\mathbf{z}_{k+1}]}, \tag{6}$$

where $\widehat{\mathfrak{z}} \in [\mathfrak{z}]$ and $[\mathbf{z}_{k+1}](\widehat{\mathfrak{z}})$ is the box obtained when integrating the system with known initial conditions taken as $\widehat{\mathfrak{z}}$. In (6),

$$\frac{\partial h_i(\mathbf{z},t_k)}{\partial \mathfrak{z}} = \begin{pmatrix} \frac{\partial z_1}{\partial \mathfrak{z}_1} & \cdots & \frac{\partial z_n}{\partial \mathfrak{z}_1} \\ \vdots & \ddots & \vdots \\ \frac{\partial z_1}{\partial \mathfrak{z}_n} & \cdots & \frac{\partial z_n}{\partial \mathfrak{z}_n} \end{pmatrix} \begin{pmatrix} \frac{\partial h_i}{\partial z_1} \\ \vdots \\ \frac{\partial h_i}{\partial z_n} \end{pmatrix}$$

where $\frac{\partial z_i}{\partial \mathfrak{z}_j}$ is the *sensitivity function* of the i-th state component with respect to the initial condition of the j-th state component.

Taking into account the measurement at time t_k,

$$h_i([\mathbf{z}_{k+1}](\widehat{\mathfrak{z}}),t_k) + ([\mathfrak{z}]-\widehat{\mathfrak{z}})^{\mathrm{T}} \left.\frac{\partial h_i(\mathbf{z},t_k)}{\partial \mathfrak{z}}\right|_{[\mathbf{z}_{k+1}]} \subset \left[y_i(t_k)-\overline{\delta}, y_i(t_k)+\overline{\delta}\right],\ i=1\ldots m.$$

Thus each $[\mathfrak{z}_i]$, $i=1\ldots n$, has to satisfy

$$[\mathfrak{z}_i] \subset \left(y(t_k) - \left[-\overline{\delta},\overline{\delta}\right] - h_i([\mathbf{z}_{k+1}](\widehat{\mathfrak{z}}),t_k) - \sum_{j\neq i}([\mathfrak{z}_j]-\widehat{\mathfrak{z}}_j)\left[\frac{\partial h_i}{\partial \mathfrak{z}_j}\right]([\mathbf{z}_{k+1}])\right) / \left[\frac{\partial h_i}{\partial \mathfrak{z}_i}\right]([\mathbf{z}_{k+1}]) + \widehat{\mathfrak{z}}_i,$$

leading to a contracted box $[\mathfrak{z}]^{\mathrm{new}} = C_i([\mathfrak{z}])$, the components of which are defined as

$$[\mathfrak{z}_i]^{\mathrm{new}} = [\mathfrak{z}_i] \cap \left(\left(y(t_k) - \left[-\overline{\delta},\overline{\delta}\right] - h_i([\mathbf{z}_{k+1}](\widehat{\mathfrak{z}}),t_k) - \sum_{j\neq i}([\mathfrak{z}_j]-\widehat{\mathfrak{z}}_j)\left[\frac{\partial h_i}{\partial \mathfrak{z}_j}\right]([\mathbf{z}_{k+1}])\right) / \left[\frac{\partial h_i}{\partial \mathfrak{z}_i}\right]([\mathbf{z}_{k+1}]) + \widehat{\mathfrak{z}}_i\right)$$

for $i=1\ldots n$.

This contractor requires the computation of an inclusion function for the sensitivity functions of each state component with respect to the initial condition; see the next section.

4.2.3 Sensitivity Functions

Denote the first-order sensitivity of z_j with respect to $\mathfrak{z}_k$ by s_{jk}

$$s_{jk}(\mathfrak{z},t) = \frac{\partial z_j}{\partial \mathfrak{z}_k}(\mathfrak{z},t).$$

Assume for simplicity that the model output is linear in the state and it is given by

$$\mathbf{h}(\mathbf{z}(t),t) = \mathbf{C}\mathbf{z}(t),$$

where $\mathbf{C} = (\mathbf{c}_1 \dots \mathbf{c}_n)^T$ is a known matrix. Then

$$\frac{\partial \mathbf{h}(\mathbf{z}(t),t)}{\partial \mathfrak{z}} = \begin{pmatrix} \mathbf{c}_1^{\mathrm{T}} \frac{\partial \mathbf{z}}{\partial \mathfrak{z}_1} \\ \vdots \\ \mathbf{c}_n^{\mathrm{T}} \frac{\partial \mathbf{z}}{\partial \mathfrak{z}_n} \end{pmatrix}.$$

Differentiate once the jth row of (1) with respect to $\mathfrak{z}_k$ to obtain the differential equation

$$\dot{s}_{jk} = \frac{\partial f_j(\mathbf{z})}{\partial z_j} s_{jk}. \tag{7}$$

Since $\mathfrak{z}$ is a scaled version of $\mathbf{z}(t_0)$, the initial conditions for the sensitivity functions are

$$s_{jk}(t_0) = \frac{\partial z_j(t_0)}{\partial \mathfrak{z}_k} = \begin{cases} d_{jj} \text{ if } j = k, \\ 0 \quad \text{else.} \end{cases}$$

The sensitivity functions may then be obtained by considering a new *extended* state-space model consisting of (1) and of all differential equations (7) satisfied by the sensitivity functions. Müller's theorem turns out to be especially useful, as the extended state-space model is seldom cooperative, even if this is the case of the initial state-space model.

4.3 Using Taylor Models

In the case of Taylor models, the correction step is quite different from what has been described in Section 4.1. The measurement equation (2), (3) is rewritten as

$$\mathbf{h}(\mathbf{z}_{k+1}) + \delta - \mathbf{y}(t_{k+1}) = 0. \tag{8}$$

Each Taylor model $\mathbf{T}_{\rho,k+1}^{(pr,l)}(\mathfrak{z})$ of $\mathscr{T}_{k+1}^{(pr)}$ is now considered separately and substituted for $\mathbf{z}_{k+1}$ in (8) to obtain

$$\mathbf{h}\left(\mathbf{T}_{\rho,k+1}^{(pr,l)}(\mathfrak{z})\right) + \delta - \mathbf{y}(t_{k+1}) = 0. \tag{9}$$

For nonlinear systems, the left hand side of (9) is nonlinear even for a linear measurement equation, since the Taylor model $\mathbf{T}^{(pr,l)}_{\rho,k+1}(\mathfrak{z})$ is nonlinear. One knows that $\delta \in [-\overline{\delta}, \overline{\delta}]$, thus, (9) may be solved for $\mathfrak{z}$ with an interval Newton method, which leads to a tightened domain interval $[\tilde{\mathfrak{z}}]$, hence $\mathfrak{z} \in [\tilde{\mathfrak{z}}]$. Here, the Krawczyk method is used. For $n > m$, (9) is under-determined and cannot be inverted. A simple approach is to solve (9) only for m variables (components of $\mathfrak{z}$), while considering the remaining $n-m$ variables as constant intervals.

This procedure is illustrated for a very simple linear example with $n = 2$ and $m = 1$. Consider the case when (9) is given by

$$\mathfrak{z}_1 + 0.5\mathfrak{z}_2 + \delta_1 - y_1(t_{k+1}) = 0, \tag{10}$$

with $[\mathfrak{z}_1] = [-1;1]$, $[\mathfrak{z}_2] = [-1;1]$, $y_1(t_{k+1}) = 0.9$, and $[\delta_1] = [-0.1;0.1]$. Now, (10) is first solved for $\mathfrak{z}_1$, the interval $[-1;1]$ being used for $\mathfrak{z}_2$. We have

$$[\tilde{\mathfrak{z}}_1] = y_1(t_{k+1}) - [\delta_1] - 0.5[\mathfrak{z}_2] = 0.9 - [-0.1;0.1] - 0.5[-1;1] = [0.3;1.5].$$

Now this result is intersected with the initial interval enclosure $[-1;1]$ resulting in

$$[\tilde{\mathfrak{z}}_1] = [0.3;1.5] \cap [-1;1] = [0.3;1].$$

Next, (10) is solved for $\mathfrak{z}_2$ with the new $[\mathfrak{z}_1]$

$$[\tilde{\mathfrak{z}}_2] = 2(y_1(t_{k+1}) - [\delta_1] - [\tilde{\mathfrak{z}}_1]) = 2(0.9 - [-0.1;0.1] - [0.3;1]) = [-0.4;1.4].$$

An intersection with the initial interval enclosure $[-1;1]$ results in

$$[\tilde{\mathfrak{z}}_2] = [-0.4;1.4] \cap [-1;1] = [-0.4;1].$$

Another possibility is to consider a sufficient number of previous measurements $\mathbf{y}(t \le t_k)$ and the corresponding Taylor models of the right hand side of (9) to obtain the missing $n-m$ equations.

If no solution in $[\mathfrak{z}]$ can be found, then the corresponding Taylor model is inconsistent with the data and can be deleted.

As previously, the Taylor model is computed for a normalized domain box and written as

$$\begin{aligned}[\tilde{\mathfrak{z}}] \in &\widetilde{\mathbf{T}}(\mathfrak{z}) = \tilde{\mathbf{c}} + \widetilde{\mathbf{D}}\,\mathfrak{z} \\ &\text{with } \mathfrak{z}_i \in [-1;1], i = 1 \ldots n,\end{aligned}$$

where $\tilde{\mathbf{c}}$ is the midpoint of $[\tilde{\mathfrak{z}}]$ and $\widetilde{\mathbf{D}}$ is a diagonal matrix with $\tilde{d}_{i,i} = \mathrm{rad}([\tilde{\mathfrak{z}}_i])$. The Taylor model $\mathbf{T}^{(c,l)}_{k+1}$ after the correction step is then given by

$$\mathbf{T}^{(c,l)}_{\rho,k+1}(\mathfrak{z}) = \mathbf{T}^{(pr,l)}_{\rho,k+1}(\widetilde{\mathbf{T}}(\mathfrak{z})),$$

which defines the l-th Taylor model for the next prediction step:

$$\mathbf{T}^{(l)}_{\rho,k+1}(\mathfrak{z}) = \mathbf{T}^{(c,l)}_{\rho,k+1}(\mathfrak{z}).$$

The list of Taylor models at $k+1$ is then given by

$$\begin{aligned}\mathbf{z}_{k+1} \in \mathscr{T}_{\rho,k+1} = &\left\{\mathbf{T}^{(1)}_{\rho,k+1}(\mathfrak{z}), \mathbf{T}^{(2)}_{\rho,k+1}(\mathfrak{z}) \dots \mathbf{T}^{(L_{k+1})}_{\rho,k+1}(\mathfrak{z})\right\} \\ &\text{with} \quad \mathfrak{z}_i = [-1;1], \quad i = 1 \dots n \quad \text{with} \quad L_{k+1} \leq L^{pr}_{k+1} \leq L_{max} \ .\end{aligned}$$

Interval Newton methods, like the Krawczyk method, involve the computation of the derivatives of $\mathbf{h}$ with respect to the initial states $\mathfrak{z}$ similar to (6) in the correction step for the method based on Müller's theorem. Since the Taylor model performs an expansion in the initial states $\mathfrak{z}$, the derivatives are easily obtained by calculating them for the Taylor model obtained from (9).

The correction step in combination with preconditioning is explained in [14], together with a correction step that involves consistency tests.

5 Simulation Results

For a comparison of the two approaches, consider the following nonlinear system

$$\begin{cases} \dot{x}_1 = -p_3 x_1 - \dfrac{p_1 x_1}{1 + p_2 x_1} + p_4 x_2 \\ \dot{x}_2 = p_3 x_1 - p_4 x_2 \end{cases}$$

with the initial value of the state $x_1(0) = 1$ and $x_2(0) = 0$.

Only x_2 is measured and the measurement equation at $t = t_k$ is

$$y_k = x_2(t_k) + \delta_k.$$

The parameters p_1, p_2 and p_3 are given by $p_1 = 1$, $p_2 = 1.2$ and $p_3 = 0.5$. The parameter p_4 is uncertain with $p_4 \in [0.1, 0.5]$. Thus, the extended state satisfies

$$\begin{cases} \dot{z}_1 = -p_3 z_1 - \dfrac{p_1 z_1}{1 + p_2 z_1} + z_3 z_2 \\ \dot{z}_2 = p_3 z_1 - z_3 z_2 \\ \dot{z}_3 = 0 \end{cases} \tag{11}$$

with $z_1 = x_1$, $z_2 = x_2$, and $z_3 = p_4$. Measurements are assumed to take place every 2 s. The measurement uncertainty is given by $\delta(t_k) \in [-0.005, 0.005]$ for all t_k.

5.1 Results with Prediction Based on Müller's Theorem

5.1.1 Correction using `Sivia`

We used the `Sivia` algorithm combined with `ImageSp` to estimate the extended state vector. For this purpose, a coupled system of ODEs is built from (11)

$$\begin{cases} \dot{\underline{z}}_1 = -p_3\underline{z}_1 - \dfrac{p_1\underline{z}_1}{1+p_2\underline{z}_1} + \underline{z}_3\underline{z}_2 \\ \dot{\underline{z}}_2 = p_3\underline{z}_1 - \bar{z}_3\underline{z}_2 \\ \dot{\underline{z}}_3 = 0 \\ \dot{\bar{z}}_1 = -p_3\bar{z}_1 - \dfrac{p_1\bar{z}_1}{1+p_2\bar{z}_1} + \bar{z}_3\bar{z}_2 \\ \dot{\bar{z}}_2 = p_3\bar{z}_1 - \underline{z}_3\bar{z}_2 \\ \dot{\bar{z}}_3 = 0 \end{cases} \tag{12}$$

with $\underline{z}_1(0) = \bar{z}_1(0) = 1$, $\underline{z}_2(0) = \bar{z}_2(0) = 0$, and $\left[\underline{z}_3(0), \bar{z}_3(0)\right]$ dependent on the iteration in `Sivia`. Using (12), an inclusion function for $h(\mathbf{z}(t_k)) = z_2(t_k)$ is obtained.

The estimates for p_4 obtained at $t = 10\ s$ using the `Sivia` algorithm for various values of the precision parameter ε are provided in Table 1. As expected, reducing ε increases the computing time and the accuracy of the estimate. These results have been obtained using a single core of a two-processor, quadri-core Intel Xeon CPU E5462 at 2.80 GHz with 6 144 KB cache and 64 GB RAM.

ε	time (s)	estimate for p_4
0.05	1.28	[0.125,0.35]
0.025	1.85	[0.1625,0.3125]
0.01	4.3	0.2[1718,8750]
0.005	8.28	0.2[3303,6875]
0.0025	15.77	0.2[4063,6251]
0.001	31.95	0.2[4546,5804]

Table 1 Estimates for p_4 obtained with `Sivia` at $t = 10\ s$ for various values of ε

5.1.2 Correction by Constraint Propagation

Since only the third initial condition is unknown, only the first-order sensitivity functions with respect to z_3 have to be evaluated. For that purpose, each ODE in (11) is derived with respect to z_3 to get

$$\begin{cases} \dot{s}_{13} = \left(-p_3 - \dfrac{p_1}{1+p_2 z_1} + \dfrac{p_1 p_2}{(1+p_2 z_1)^2} \right) s_{13} + s_{33} z_2 + z_3 s_{23} \\ \dot{s}_{23} = p_3 s_{13} - s_{33} z_2 - z_3 s_{23} \\ \dot{s}_{33} = 0 \end{cases} \tag{13}$$

with $s_{13}(0) = s_{23}(0) = 0$ and $s_{33}(0) = 1$. Müller's theorem may be used with (13) to compute an enclosure of the sensitivity function of the state with respect to the third initial condition, which is also p_4

$$\begin{cases} \dot{\underline{s}}_{13} = \left(-p_3 - \dfrac{p_1}{1+p_2 \underline{z}_1} + \dfrac{p_1 p_2 \underline{z}_1}{(1+p_2 \overline{z}_1)^2} \right) \underline{s}_{13} + \underline{z}_2 \underline{s}_{33} + \overline{z}_3 \underline{s}_{23} \\ \dot{\underline{s}}_{23} = p_3 \underline{s}_{13} - \overline{s}_{33} \overline{z}_2 - \underline{z}_3 \underline{s}_{23} \\ \dot{\underline{s}}_{33} = 0 \\ \dot{\overline{s}}_{13} = \left(-p_3 - \dfrac{p_1}{1+p_2 \overline{z}_1} + \dfrac{p_1 p_2 \overline{z}_1}{\left(1+p_2 \underline{z}_1\right)^2} \right) \overline{s}_{13} + \overline{s}_{33} \overline{z}_2 + \underline{z}_3 \overline{s}_{23} \\ \dot{\overline{s}}_{23} = p_3 \overline{s}_{13} - \underline{s}_{33} \underline{z}_2 - \overline{z}_3 \overline{s}_{23} \\ \dot{\overline{s}}_{33} = 0 \end{cases}$$

This enclosure uses the fact that all quantities are positive, except $s_{23}(t) \leq 0$ for $t \geq 0$. The contractor described in Section 4.2 may then be employed in conjunction with `Sivia` to reduce the uncertainty on the initial value of the third component of the state.

Table 2 describes the evolution with time of the estimate for p_4 as a function of the precision parameter ε. Reducing ε again increases the accuracy at which the estimate is obtained, but the price to be paid is an increased complexity, since more ODEs are solved. Contrary to `Sivia`, a decent estimate is obtained even with the largest value of ε. The first and second measurements provide the most information about p_4, since for these measurements, the best decrease in the size of $[z_3]$ is observed. See also Figure 1. The same processor as in Section 5.1.1 has been used here.

Time	$\varepsilon = 0.2$	$\varepsilon = 0.1$	$\varepsilon = 0.05$	$\varepsilon = 0.01$
2 s	0.2[20488,57674]	0.2[24304,57668]	0.2[23906,57668]	0.2[24323,56828]
4 s	0.2[30813,57674]	0.2[34575,57668]	0.2[35411,57668]	0.2[40556,56828]
6 s	0.2[30813,57674]	0.2[36483,57668]	0.2[37597,57668]	0.2[44613,56828]
8 s	0.2[30813,57674]	0.2[36483,57668]	0.2[37597,57668]	0.2[44613,56828]
10 s	0.2[30813,57674]	0.2[36483,57668]	0.2[37597,57668]	0.2[44613,56250]
Comp.	1.0 s	2.13 s	3.47 s	17 s

Table 2 Evolution of the estimate for p_4 with `Sivia` for various values of the precision parameter ε as a function of the time and total computing time

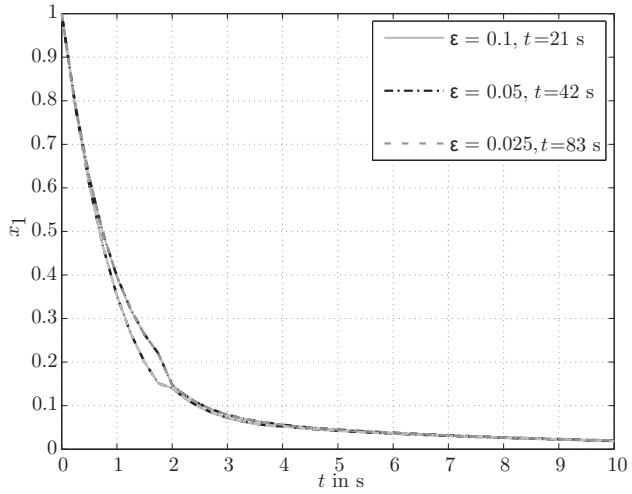

(a) Estimation of x_1

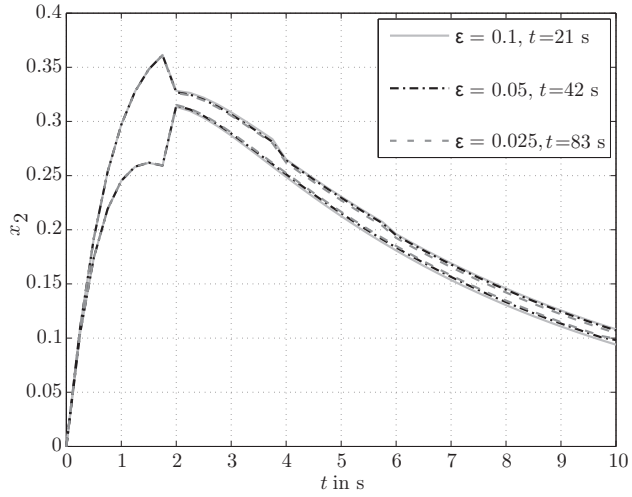

(b) Estimation of x_2

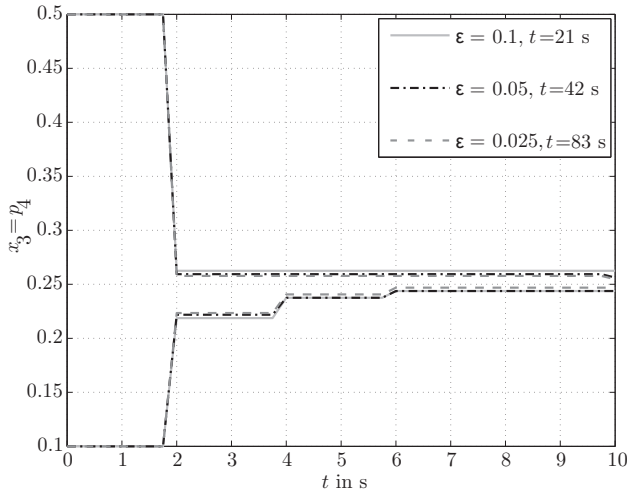

(c) Estimation of p_4

Fig. 1 Comparison of the estimation results with `Sivia` for different values of the precision parameter ε used in the Müller method

5.2 Prediction and Correction Involving Taylor Models

Estimation results for the approach based on Taylor models are shown for different orders and numbers L_{max} of Taylor models. In Figure 2 results for $\rho = 4$, $\rho = 6$, and $\rho = 12$ for a single Taylor model ($L_{max} = 1$, hence without splitting of the domain box) are depicted together with one result for $\rho = 5$ with 4 Taylor models ($L_{max} = 4$), hence with splitting of the domain box. In this section, all computations have been done on a Intel Centrino Core2 Duo T7300 at 2 GHz. In Table 3 the interval enclosures for the evolution of the estimate for p_4 as a function of time and total computing time are given. In Table 4 the interval enclosures for the estimated parameter p_4 at $t = 10$ s for various orders and numbers of Taylor models are presented. Increasing the order from 4 to 6 leads to an improvement with a slightly

Time t	$\rho = 4, L_{max} = 1$	$\rho = 6, L_{max} = 1$	$\rho = 12, L_{max} = 1$	$\rho = 5, L_{max} = 4$
2 s	0.2[07577 ,73053]	0.2[15534 ,65326]	0.2[15721 ,65149]	0.2[23622 ,57193]
4 s	0.2[33970 ,69719]	0.2[41587 ,62131]	0.2[41710 ,62005]	0.2[41941 ,57194]
6 s	0.2[33758 ,69931]	0.2[41585 ,62133]	0.2[41710 ,62005]	0.2[41941 ,57194]
8 s	0.2[40235 ,70064]	0.2[47399 ,62134]	0.2[47508 ,62005]	0.2[47786 ,57194]
10 s	0.2[40111 ,60466]	0.2[47399 ,53480]	0.2[47508 ,53377]	0.2[47786 ,53354]
Comp.	0.87 s	1.12 s	4.83 s	3.51 s

Table 3 Evolution of the estimate for p_4 for various values of ρ and L_{max} as a function of time, and total computing time

ρ	L_{max}	comp. time (s)	estimate for p_4
4	1	0.87	0.2[40111,60466]
6	1	1.12	0.2[47399,53480]
12	1	4.83	0.2[47508,53377]
5	4	3.51	0.2[47786,53354]

Table 4 Estimates obtained with Talyor models at $t = 10$ s for various values of ρ and numbers of Taylor models.

higher computation time. However if the order is increased to 12, the computation time increases drastically (from 1.12s to 4.83s) without tightening the enclosures in any significant manner. Further improvement of the estimation results is achieved only if splitting is applied as the results for $\rho = 5$ and $L_{max} = 4$ indicate. Even the computation time is lower than for $\rho = 12$ and $L_{max} = 1$.

6 Conclusions and Perspectives

Physics, chemistry (and most other experimental sciences) tend to produce continuous-time models whose outputs are nonlinear in their unknown parameters. When these

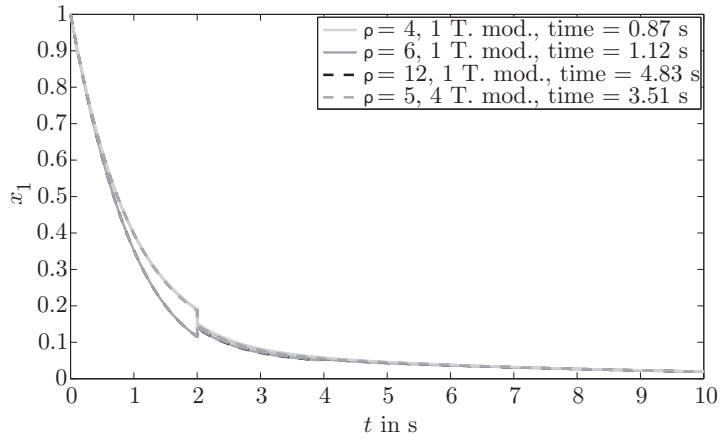

(a) Estimation of x_1

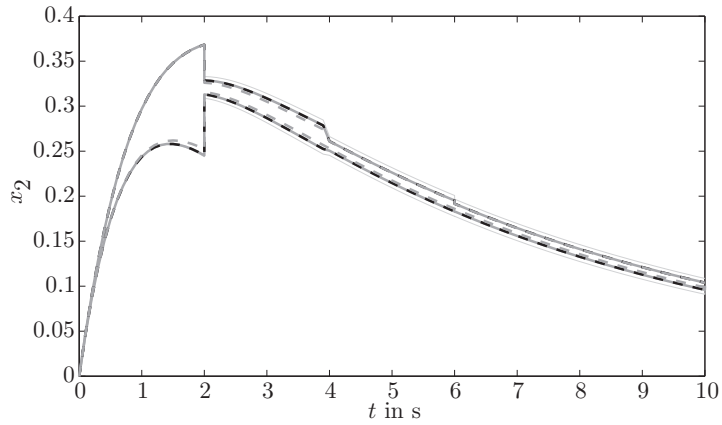

(b) Estimation of x_2

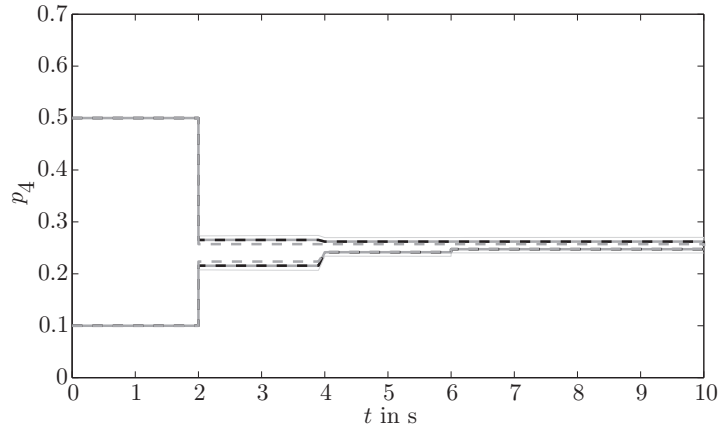

(c) Estimation of p_4

Fig. 2 Comparison of the estimation results for different orders and number of Taylor models.

models are in state-space form, they are almost always nonlinear in the extended state vector obtained by concatenating the state and parameter vectors. Most of the methods available for estimating this extended state vector are based on linearization or random exploration and cannot provide any guarantee as to their results. Since each of the parameters and state variables of such models has a concrete physical meaning, this is unfortunate. One would rather like to be able to characterize in some guaranteed way the set of all acceptable estimates given what is known of the uncertainty in the experimental data.

For quite some time, this has been completely out of reach, but a combination of advances in interval analysis, constraint propagation, and guaranteed integration of ODEs, together with a massive increase in computing power have now made this achievable, at least for small-scale models. This paper has presented, in a coordinated manner, a variety of tools that can be used when bounds are available on the acceptable difference between the data and corresponding model output.

Guaranteed set estimation makes it possible to bypass the usual requirements of identifiability, observability, and persistency of excitation. These properties should nevertheless definitely contribute to the quality of the parameter and state estimates. More generally, the problem of experiment design for guaranteed parameter or state estimation is an interesting but still largely open question.

The main challenge is to increase the complexity of the models that can be studied with this type of guaranteed approach. To this end, it is necessary to use and possibly combine tools that struggle as efficiently as possible with the pessimism inherent to interval analysis and guaranteed integration and the curse of dimensionality. Contractors, which make it possible to eliminate parts of the search region without the need for bisections, and high-order Taylor models are among the most promising avenues for research.

References

1. Berz, M., Makino, K.: Verified integration of ODEs and flows using differential algebraic methods on high-order Taylor models. Reliable Computing **4**, 361–369 (1998)
2. Chernousko, F.L.: Optimal guaranteed estimates of indeterminacies with the aid of ellipsoids. Engrg. Cybernetics **18**, 1–9 (1980)
3. Chernousko, F.L.: State Estimation for Dynamic Systems. CRC Press, Boca Raton, FL (1994)
4. Gennat, M., Tibken, B.: Simulation of uncertain systems with guaranteed bounds. In: 11th GAMM - IMACS International Symposium on Scientific Computing, Computer Arithmetic, and Validated Numerics. Fukuoka, Japan (2004)
5. Gouzé, J.L., Rapaport, A., Hadj-Sadok, Z.M.: Interval observers for uncertain biological systems. Journal of Ecological Modelling (133), 45–56 (2000)
6. Hoefkens, J., Berz, M., Makino, K.: Efficient high-order methods for ODEs and DAEs. In: G. Corliss, C. Faure, A. Griewank (eds.) Automatic Differentiation : From Simulation to Optimization, pp. 341–351. Springer-Verlag, New-York, NY (2001)
7. Jaulin, L.: Nonlinear bounded-error state estimation of continuous-time systems. Automatica **38**, 1079–1082 (2002)
8. Jaulin, L., Kieffer, M., Didrit, O., Walter, E.: Applied Interval Analysis. Springer-Verlag, London (2001)

9. Jaulin, L., Walter, E.: Set inversion via interval analysis for nonlinear bounded-error estimation. Automatica **29**(4), 1053–1064 (1993)
10. Kieffer, M., Walter, E.: Guaranteed parameter estimation for cooperative systems. In: L. Benvenuti, A. De Santis, L. Farina (eds.) Positive Systems – LNCIS 294, pp. 103–110. Springer, Berlin (2003)
11. Kieffer, M., Walter, E.: Interval analysis for guaranteed nonlinear parameter and state estimation. Mathematical and Computer Modelling of Dynamic Systems **11**(2), 171–181 (2005)
12. Kieffer, M., Walter, E.: Guaranteed nonlinear state estimation for continuous–time dynamical models from discrete–time measurements. In: Preprints of the 5th IFAC Symposium on Robust Control Design (2006)
13. Kieffer, M., Walter, E.: Guaranteed estimation of the parameters of nonlinear continuous–time models: contributions of interval analysis. Int. J. Adap. Contr. Sig. Proc. (2010). Doi : 10.1002/acs.1194
14. Kletting, M.: Verified Methods for State and Parameter Estimators for Nonlinear Uncertain Systems with Applications in Engineering. Ph.D. thesis, Institute of Measurement, Control, and Microtechnology,University of Ulm, Germany (2009)
15. Kühn, W.: Rigorously computed orbits of dynamical systems without the wrapping effect. Computing **61**(1), 47–67 (1998)
16. Kurzhanski, A., Valyi, I.: Ellipsoidal Calculus for Estimation and Control. Birkhäuser, Boston, MA (1997)
17. Lin, Y., Stadtherr, M.A.: Validated solution of ODEs with parametric uncertainties. In: W. Marquardt, C. Pantelides (eds.) Proc. 16th European Symposium on Computer Aided Process Engineering and 9th International Symposium on Process Systems Engineering, *Computer Aided Chemical Engineering*, vol. 21, pp. 167 – 172. Elsevier (2006). DOI 10.1016/S1570-7946(06)80041-6. URL `http://www.sciencedirect.com/science/article/B8G5G-4P37F2K-S/2/a22680956d2786784b23e88e9b272db6`
18. Lohner, R.: Computation of guaranteed enclosures for the solutions of ordinary initial and boundary value-problem. In: J.R. Cash, I. Gladwell (eds.) Computational Ordinary Differential Equations, pp. 425–435. Clarendon Press, Oxford (1992)
19. Makino, K., Berz, M.: Suppression of the wrapping effect by Taylor model-based verified integrators: Long-term stabilization by preconditioning. International Journal of Differential Equations and Applications **10**(4), 353–384 (2005)
20. Makino, K., Berz, M.: Suppression of the wrapping effect by Taylor model-based verified integrators: Long-term stabilization by shrink wrapping. International Journal of Differential Equations and Applications **10**(4), 385–403 (2005)
21. Meslem, N., Ramdani, N., Candau, Y.: Guaranteed state bounding estimation for uncertain non linear continuous systems using hybrid automata. In: Proc. IFAC International Conference on Informatics in Control, Automation Robotics. Funchal, Madeira (2008)
22. Meslem, N., Ramdani, N., Candau, Y.: Interval observers for uncertain nonlinear systems. application to bioreactors. In: Proc. IFAC World Congress, pp. 9667–9672. Seoul, Korea (2008)
23. Moisan, M., Bernard, O., Gouz, J.L.: Near optimal interval observers bundle for uncertain bioreactors. Automatica **45**(1), 291–295 (2009)
24. Müller, M.: Über das Fundamentaltheorem in der Theorie der gewöhnlichen Differentialgleichungen. Math. Z. **26**, 619–645 (1926)
25. Nedialkov, N.S., Jackson, K.R.: Methods for initial value problems for ordinary differential equations. In: U. Kulisch, R. Lohner, A. Facius (eds.) Perspectives on Enclosure Methods, pp. 219–264. Springer-Verlag, Vienna (2001)
26. Raissi, T., Ramdani, N., Candau, Y.: Set membership state and parameter estimation for systems described by nonlinear differential equations. Automatica **40**(10), 1771–1777 (2004)
27. Raissi, T., Videau, G., Zolghadri, A.: Interval observer design for consistency checks of nonlinear continuous-time systems. Automatica **46**(3), 518–527 (2010)
28. Rauh, A., Auer, E., Minisini, J., Hofer, E.P.: Extensions of ValEncIA-IVP for reduction of overestimation, for simulation of differential algebraic systems, and for dynamical optimization. Proc. Appl. Math. Mech. **7**(1), 1023,0011023,002 (2007). DOI 10.1002/pamm.200700022

29. Rauh, A., Hofer, E.P., Auer, E.: VALENCIA-IVP: A comparison with other initial value problem solvers. In: Proc. 12th GAMM - IMACS International Symposium on Scientific Computing, Computer Arithmetic and Validated Numerics (SCAN 2006), p. 36. IEEE Computer Society, Duisburg, Germany (2006). DOI 10.1109/SCAN.2006.47
30. Veres, S.M., Mayne, D.Q.: Geometric bounding toolbox. Tech. rep. URL `http://www.sysbrain.com/gbt/`
31. Walter, E., Kieffer, M.: Interval analysis for guaranteed nonlinear estimation. In: Proceedings of the 13th IFAC Symposium on System Identification (SYSID), pp. 259–270 (2003)
32. Walter, E., Kieffer, M.: Guaranteed nonlinear parameter estimation in knowledge–based models. Journal of Computational and Applied Mathematics **199**(2), 277–285 (2007)